

# Reversible magnetization processes and energy density product in Sm–CoFe and Sm–Co/Co bilayers

T. Schrefl,<sup>a)</sup> H. Forster, R. Dittrich, D. Suess, W. Scholz, and J. Fidler

*Solid State Physics, Vienna University of Technology, Wiedner Haupstr. 8-10/138, A-1040 Vienna, Austria*

(Presented on 12 November 2002)

The hysteresis properties of epitaxial SmCo/Co and SmCo/Fe bilayers are calculated by the solution of the Landau–Lifshitz Gilbert equation. The thin film grain structure is taken into account using appropriate finite element techniques. The  $J(H)$  curve shows the typical exchange spring behavior for the bilayer if the soft magnetic layer thickness exceeds 10 nm. However, the reversible rotations of the magnetization for low external field deteriorate the maximum energy density product. Straight  $B(H)$  curves are obtained only for a Fe layer thickness of 5 nm. Magnetization reversal starts with the reversible rotation of the soft layer magnetization. Initially, the magnetization rotates in opposite directions in different regions of the film. The reversible rotations penetrate substantially into the hard layer. © 2003 American Institute of Physics. [DOI: 10.1063/1.1558245]

## I. INTRODUCTION

Nanostructured permanent magnets have great potential for micro-electromechanical systems (MEMS) application, since it is possible to tailor their magnetic properties according to the specific requirements. A prominent example for nanostructured permanent magnets are hard magnetic/soft magnetic bilayers. They also provide an excellent model system to study fundamental magnetization processes both experimentally and numerically. The so-called exchange spring mechanism, originally proposed by Kneller and Hawig,<sup>1</sup> forms the basis of two-phase permanent magnets. A mixture of a magnetically hard phase and a magnetically soft phase shows excellent hard magnetic properties provided that both phases are exchange coupled. Owing to the exchange interactions between the hard and the soft magnetic phase the magnetization reversal process is reversal up to high opposing external fields. The magnetic polarization of the soft magnetic phase rotates reversibly out of its easy direction, which is parallel to the anisotropy direction of the adjacent hard phase, if a sufficiently large inverse magnetic field is applied. Within the soft magnetic phase the magnetization shows a twist with gradually rotating magnetization. The rotation angle increases with increasing distance from the hard phase, as schematically shown in Fig. 1 for a hard magnetic/soft magnetic bilayer. The magnetization forms a Bloch wall like structure and will rotate back in alignment with the hard phase when the applied field is reduced. Recent experiments investigate the magnetization structure near magnetically hard/soft interfaces under an influence of an opposing field.

(1) In hard magnetic/soft magnetic bilayers, the soft magnetic layer breaks up into domains with opposite spin twist during the reversible part of the demagnetization process.<sup>2</sup>

(2) Spin-polarized neutron reflectometry<sup>3</sup> shows that the reversible twist of the magnetization penetrates considerably into the hard magnetic layer.

(3) Pollman and co-workers<sup>4</sup> investigated the domain structure of a buried SmCo layer in SmCo/Fe spring magnet using x-ray magnetic circular dichroism. The magnetic images showed domain walls not oriented parallel to the easy axis of magnetization but at angles between 45° and 90°.

In this article we compare the results of numerical micromagnetic simulations with the recent experimental findings mentioned earlier. The simulations use the finite element method<sup>5</sup> to model the granular structure of the bilayer films. The hard magnetic properties of nanocomposite magnets sensitively depend on microstructural features.<sup>6</sup> Thin film growth techniques permit the preparation of artificial nanodisperse magnetic structures. Magnetron sputtering techniques enable to control the microstructure, the crystallographic orientation, and the magnetic anisotropy of multilayer hard magnetic/soft magnetic structures.<sup>7</sup> Finite element models of bilayer structures can be built more accurately than those of bulk systems. Indeed, the numerical results are in good qualitative agreement with recent experimental work.<sup>2–4</sup> Section II introduces the numerical techniques and the finite element model of the investigated bilayer structures. Section III presents the magnetic properties calculated for SmCo/Co bilayers and SmCo/Fe bilayers.

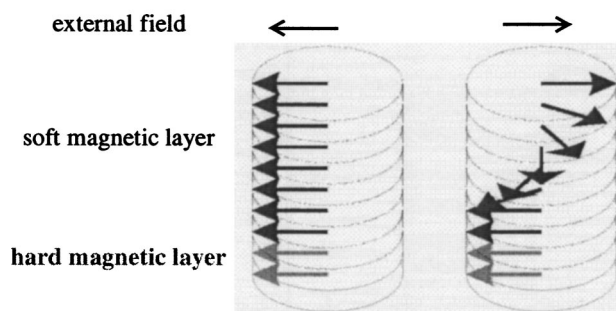


FIG. 1. The magnetization twist in an exchange spring bilayer. A reversed field larger than the absolute value of the nucleation field starts induces a gradually rotating magnetization within the soft layer.

<sup>a)</sup>Electronic mail: thomas.schrefl@tuwien.ac.at

TABLE I. Intrinsic magnetic properties used for the calculations. For  $\alpha$ -Fe zero magnetocrystalline anisotropy was assumed in the calculations.

	$K_1$ (MJ/m <sup>3</sup> )	$J_s$ (T)	$A$ (pJ/m)	Reference
SmCo <sub>5</sub>	17	1.07	8.6	9, 10
Sm <sub>2</sub> Co <sub>7</sub> , SmCo <sub>3</sub>	12	1.07	8.6	
Co	0.45	1.76	13	11
$\alpha$ -Fe	0	2.15	25	1

## II. FINITE ELEMENT MODELS

Benaissa and co-workers<sup>8</sup> investigated the structure of SmCo films grown on MgO substrates using high resolution transmission electron microscopy. The grains of (1 $\bar{1}$ 00)-oriented SmCo, grown on MgO(110) substrates, have in-plane  $c$  axes which are parallel to each other, resulting in a uniaxial structure. The studies show that the SmCo film consists of a mixture of SmCo<sub>3</sub>, Sm<sub>2</sub>Co<sub>7</sub>, and SmCo<sub>5</sub> polytypoids. The magnetocrystalline anisotropy directions of the different phases are in the plane of the film and parallel to each other. In the finite element model of the SmCo layer we have to represent the granular structure and the change of the anisotropy from grain to grain. A Voronoi construction is used to generate the grain structure of the finite element model. We randomly varied the magnetocrystalline anisotropy constant from grain to grain, assuming 50 vol% SmCo<sub>5</sub>, 25 vol% SmCo<sub>3</sub>, and 25 vol% Sm<sub>2</sub>Co<sub>7</sub>. Table I summarizes the intrinsic magnetic properties used for the calculations. The soft layer is assumed to be continuous without any structural inhomogeneities. Perfect exchange coupling is assumed at the interface between the hard and the soft layer boundary. The variation of the total Gibbs' free energy provides the interface condition at boundary between the hard layer mesh and the soft layer mesh.<sup>12</sup>

Then the grains are further subdivided into tetrahedral finite elements. In order to resolve the relevant magnetization processes, the mesh size has to be smaller than the domain wall width in the hard phase ( $\sim 2.5$  nm) and has to be equal to the exchange length in the soft phase ( $\sim 5$  nm). To reduce the computational effort we reduce the lateral size of the film to  $5 \times 5$  grains with a diameter of 30 nm. The total number of finite elements reaches 350 000. We derive a system of exchange and magnetostatically coupled magnetic moments,

assigning a magnetic moment to each node of the finite element mesh. For each magnetic moment the Landau–Lifshitz Gilbert (LLG) equation is solved. Since we are only interested in static properties the Gilbert damping parameter is set to  $\alpha = 1$ . Owing to the exchange and the magnetostatic interactions between the magnetic moments, a system of coupled nonlinear differential equations has to be solved. A preconditioned, backward differentiation time integration scheme proved to be highly efficient to solve the dynamic micromagnetic equations of irregular magnetic structures.<sup>13</sup> Initially the magnetic system is saturated parallel to the applied field direction. Then the LLG equation is integrated until equilibrium for decreasing applied field. Thus the quasistatic demagnetization curve can be obtained numerically. The magnetostatic interactions are calculated using a hybrid finite element/boundary element method.<sup>14</sup> A hierarchical multi-level method<sup>15</sup> is used to accelerate the boundary element method and to avoid the storage of the fully populated boundary element matrix.

## III. RESULTS

Figure 2 shows the calculated demagnetization curves and corresponding  $BH$  loop of 10 nm SmCo/10 nm Co and of 10 nm SmCo/5 nm Co. The shape of the demagnetization curves agrees well with experimental data<sup>7</sup> and has to be attributed to reversible rotations within the soft magnetic layer. At small inverse fields exchange interactions between the uniaxial SmCo film and the Co layer keep the Co moments parallel to the  $c$  axis of the SmCo film. When the external field reaches the nucleation field, a magnetization twist is introduced into the soft layer which corresponds to the sharp drop of the magnetic polarization during reversal. If the nucleation field  $|H_N|$  is smaller than  $J_s/\mu_0$  the second quadrant of the  $BH$  loop is no straight line but shows a knee at the nucleation field. For the 10 nm SmCo/10 nm Co bilayer the nucleation field is smaller than  $J_s/(2\mu_0)$  and the maximum possible energy density product of  $J_s^2/(4\mu_0)$  cannot be reached. The reversible rotations of the Co moments limit the energy density product. The  $(BH)_{\max}$  of 389 kJ/m<sup>3</sup> is slightly lower than the maximum possible value of 396 kJ/m<sup>3</sup>. Perfect exchange hardening can be achieved if the Co layer thickness is reduced to 5 nm. The Co layer remains stable up to an external field of  $H_{\text{ext}} = -1.45$  MA/m. How-

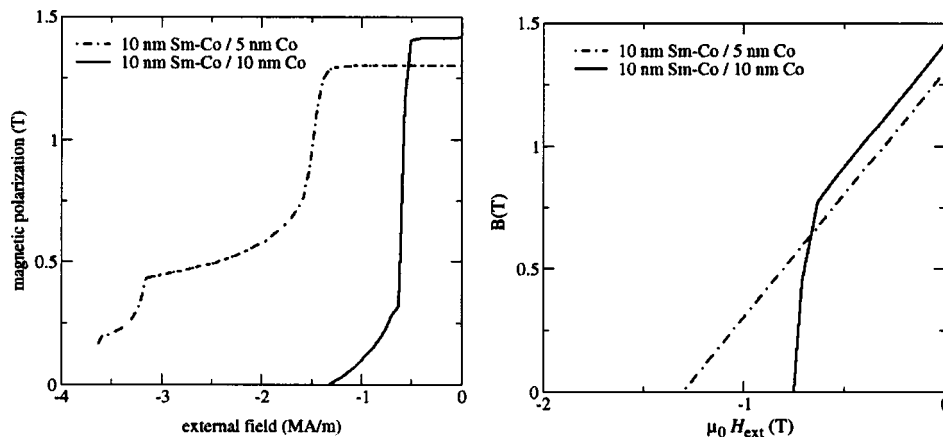


FIG. 2. Left panel: Demagnetization curves of SmCo/Co bilayers. Right panel: Second quadrant of the  $BH$  loop of SmCo/Co bilayers.

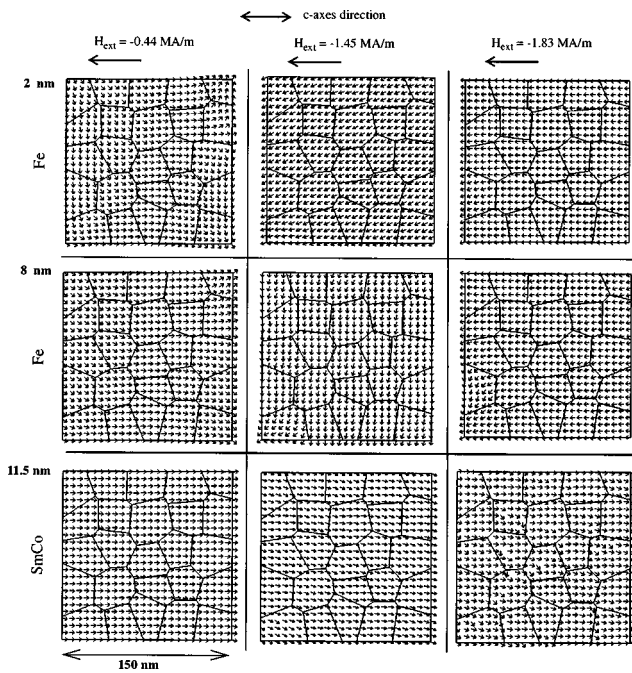


FIG. 3. Magnetization twist in a 10 nm SmCo/10 nm Fe bilayer. The plots give the magnetization configuration in a depth of 2, 8, and 11.5 nm from the top surface of the soft layer. The last slice (11.5 nm) is within the hard layer at a distance of 1.5 nm from the hard/soft interface. From left to right the opposing field is increased.

ever, the reduced saturation polarization causes a reduction of the maximum energy density product to  $(BH)_{\max} = 339 \text{ kJ/m}^3$ . Nevertheless, the calculations show that a Co layer of 5 nm thickness is sufficient to increase the energy density product considerable with respect to the single layer uniaxial SmCo film.

The highest energy density products are obtained in SmCo/Fe bilayers due to the high saturation polarization of  $\alpha$ -Fe. The energy density product increases from 390 to 405  $\text{kJ/m}^3$  if the Fe layer thickness is decreased from 10 to 5 nm. Figure 3 shows the reversible rotation of the magnetization in a 10 nm SmCo/10 nm Fe bilayer. Initially, the magnetization rotates in opposite directions in different regions of the Fe layer. The lateral extension of these regions may span several grains. With increasing rotation angle the exchange energy between the different regions becomes too large and the magnetization spontaneously switches within the smaller region to the twist direction of the large region and the soft magnetic moments become aligned almost parallel to each other. At this value of the external field the magnetization of the soft layer shows already a substantial twist. The reversible rotations penetrate substantially into the hard layer. Magnetization angles up to  $30^\circ$  with respect to the easy axis are found in a depth of 1.5 nm

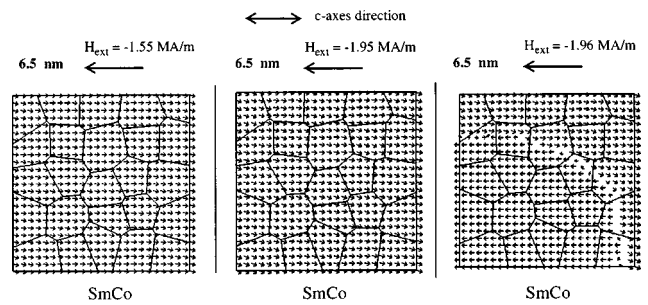


FIG. 4. Magnetization reversal in the hard layer of a 2.5 nm SmCo/5 nm Fe bilayer. The plots give the magnetization configuration in a depth of 6.5 nm from the top surface of the soft layer, thus the slices are within the hard layer at a distance of 1.5 nm from the hard/soft interface. Irreversible switching occurs at  $H_{\text{ext}} = -1.96 \text{ MA/m}$ .

The micromagnetic simulations show that multidomain states may form in the SmCo layer after an irreversible switching event. Figure 4 shows the domain formation during irreversible switching of the hard layer of a 2.5 nm SmCo/5 nm Fe bilayer. Similar magnetization processes also occur for larger SmCo thicknesses. The right-most image is a transient magnetic state obtained during the expansion of a reversed domain within the hard magnetic layer. The domain walls are oriented at angles between  $45^\circ$  and  $90^\circ$  with respect to the easy direction.

#### ACKNOWLEDGMENT

This work is supported by the Austrian Science Fund (Y-132 PHY).

- <sup>1</sup>E. F. Kneller and R. Hawig, IEEE Trans. Magn. **27**, 3588 (1991).
- <sup>2</sup>V. S. Gornakov, V. I. Nikitenko, A. J. Shapiro, R. D. Shull, J. S. Jiang, and S. D. Bader, J. Magn. Magn. Mater. **246**, 80 (2002).
- <sup>3</sup>K. V. O'Donovan, J. A. Borchers, C. F. Majrzak, O. Hellwig, and E. E. Fullerton, Phys. Rev. Lett. **88**, 67201 (2002).
- <sup>4</sup>J. Pollmann, G. Srajer, D. Hakel, J. C. Lang, J. Maser, J. S. Jiang, and S. D. Bader, J. Appl. Phys. **89**, 7165 (2001).
- <sup>5</sup>R. W. Chantrell, J. Fidler, T. Schrefl, and M. Wongsam, Encyclopedia of Materials: Science and Technology (Elsevier, Amsterdam, 2001), pp. 5651–5661.
- <sup>6</sup>J. Bernardi, T. Schrefl, J. Fidler, T. Rijks, K. de Kort, V. Archambault, D. Pere, S. David, D. Givord, J. F. Sullivan, P. Smith, J. M. D. Coey, U. Czernik, and M. Grönefeld, J. Magn. Magn. Mater. **19**, 186 (2000).
- <sup>7</sup>E. E. Fullerton, J. S. Jiang, and S. D. Bader, J. Magn. Magn. Mater. **200**, 392 (1999).
- <sup>8</sup>M. Benaissa, K. M. Krishnan, E. E. Fullerton, and J. S. Jiang, IEEE Trans. Magn. **34**, 1204 (1998).
- <sup>9</sup>E. Lectard, C. H. Allibert, and R. Ballou, J. Appl. Phys. **75**, 6277 (1994).
- <sup>10</sup>R. Skomski and J. M. D. Coey, Permanent Magnetism (IOP, Bristol, 1999).
- <sup>11</sup>W. Yang, D. N. Lambeth, and D. E. Laughlin, J. Appl. Phys. **87**, 6884 (2000).
- <sup>12</sup>H. Kronmüller and H. R. Hilzinger, J. Magn. Magn. Mater. **2**, 3 (1976).
- <sup>13</sup>D. Suess, V. Tsiantos, T. Schrefl, J. Fidler, W. Scholz, H. Forster, R. Ditzsch, and J. J. Miles, J. Magn. Magn. Mater. **248**, 298 (2002).
- <sup>14</sup>D. R. Fredkin and T. R. Koehler, IEEE Trans. Magn. **26**, 415 (1990).
- <sup>15</sup>J. Barnes and P. Hut, Nature (London) **324**, 446 (1986).